RSC Pharmaceutics

ROYAL SOCIETY OF CHEMISTRY

PAPER

View Article Online
View Journal | View Issue

Cite this: *RSC Pharm.*, 2026, **3**, 423

A bioinspired, pH-responsive microsphere matrix of cold-water extracted *Colocasia esculenta* mucilage and alginate: a new approach for sustained oral delivery of tramadol

Shazia Noureen,[a,b] Sobia Noreen,*[a,c] Fozia Batool,[a] Shazia Akram Ghumman,[d] Sara Hasan,[e,f] Samina Aslam[g] and Nisar Ahmed*[c]

Natural polymers derived from plant mucilages are increasingly explored as release-modifying agents in advanced drug delivery systems. This study presents an innovative approach utilizing cold-water extraction and ethanol precipitation to obtain *Colocasia esculenta* mucilage (CEM), which was then used to fabricate Tramadol hydrochloride-loaded microspheres *via* ionic gelation. A three-level, two-factor central composite design was employed to optimize a cross-linked CEM–alginate matrix, using polymer concentrations as independent variables, and particle size and encapsulation efficiency as response parameters. The optimized formulation exhibited stable, spherical microspheres with pH-responsive swelling and degradation behavior, high encapsulation efficiency (90.10%), and an average particle size of 726 μm. Characterization by FTIR, DSC, and XRD confirmed drug–polymer compatibility, while SEM analysis revealed a rough, wrinkled surface with fine pores. *In vitro* studies demonstrated pH-dependent drug release, achieving 67.30% release over 12 hours. *In vivo* evaluations in rabbits confirmed the formulation's safety, improved bioavailability, and prolonged gastrointestinal residence time. These results highlight the potential of cold-extracted CEM–alginate microspheres as a biocompatible, pH-responsive platform for sustained oral delivery of Tramadol. Furthermore, the simplicity and reproducibility of the ionic gelation method indicate good potential for formulation scalability, and future studies may explore the applicability of this CEM–alginate platform for other therapeutic agents requiring sustained oral delivery.

Received 24th September 2025,
Accepted 22nd January 2026

DOI: 10.1039/d5pm00263j

rsc.li/RSCPharma

Introduction

Advances in drug delivery over the past few decades have been significant but represent only a fraction of what's possible. With rising life expectancy and long-term care needs, innovative technologies are needed to address challenges like poor drug solubility, biological barriers, and the need for long-acting formulations. Learning from past experiences and supporting diverse approaches is crucial to overcome future challenges.[1] Innovative delivery platforms aim to improve drug efficacy, safety, and patient compliance by enabling targeted, controlled, and sustained delivery. Unlike traditional systems, advanced drug delivery platforms integrate innovative technologies and dosage forms to meet the body's specific needs and enable real-time monitoring. Their primary aim is to achieve optimal pharmacological efficacy with minimal side effects.[2] The success of these systems depends on early patient involvement, minimization of toxicity, enhanced therapeutic efficacy, and alignment with both commercial and therapeutic goals.[3]

The convergence of polymer and pharmaceutical sciences has facilitated the development of sophisticated drug delivery systems with controlled-release capability, biodegradability, and bioadhesion. This progress highlights key considerations in the selection and design of polymers for biomedical applications.[4,5] Polymeric drug delivery systems, whether as formulations or devices, enable the effective administration of therapeutic agents and increasingly incorporate eco-friendly and biodegradable polymers due to their superior biocompatibility and functional versatility. Continued research is essential to translate these innovations into practical clinical applications.[6,7]

Natural polymers extracted from mucilages are gaining attention in pharmaceutical formulations to craft release-mod-

[a]*Institute of Chemistry, University of Sargodha, Sargodha-40100, Pakistan*
[b]*Higher Education Department, Punjab, Pakistan*
[c]*Centre for Advanced Green Technologies and Innovation (CAGTI), Cardiff, CF23 5DT, UK. E-mail: sobia.noreen@uos.edu.pk, nisarhej@gmail.com*
[d]*College of Pharmacy, University of Sargodha, Sargodha-40100, Pakistan*
[e]*School of Chemistry and Physics, Science and Engineering Faculty, Queensland University of Technology, Brisbane, QLD, 4000, Australia*
[f]*Department of Chemistry, The University of Lahore, Sargodha Campus, Sargodha, 40100, Pakistan*
[g]*Department of Chemistry, The Women University Multan, Multan-60000, Pakistan*

ifying agents in both conventional and advanced drug delivery systems. Their unique swelling properties enable controlled or rapid drug release, depending on concentration and formulation.[8,9] Their distinctive physicochemical properties and biocompatibility have attracted interest for applications in advanced drug delivery, gene therapy, and biosynthesis, supported by ongoing modifications to enhance performance and safety.[10,11] The yield, functional, and rheological properties of mucilage are strongly influenced by the extraction method and conditions. Maceration followed by precipitation is the common approach, with hot water and low solid–liquid ratios often used. Water-extracted mucilage typically exhibits higher viscosity; however, all extraction methods may result in protein contamination, which can affect purity and stability. Elevated temperature and prolonged extraction increase protein content and discoloration of the mucilage, thereby limiting its industrial applicability.[12]

Colocasia esculenta corms are rich in mucilage with promising pharmaceutical applications and primarily consist of carbohydrates, with galactose, arabinose, glucose, and mannose as the dominant sugars. Chemically, *Colocasia esculenta* mucilage (CEM) is a naturally occurring heteropolysaccharide composed of these monosaccharide units arranged in a branched polymeric network. Due to its binding, emulsifying, suspending, and mucoadhesiveness, attributed to its slightly acidic pH, good flowability, and notable water absorption capacity, CEM has been explored as a functional excipient in controlled-release formulations and novel drug delivery systems.[13] The polysaccharide chains of CEM contain abundant hydroxyl (–OH) and carboxyl (–COOH) functional groups, which contribute to its hydrophilicity, swelling behavior, and ability to interact with other polymers and multivalent ions. Previous studies have shown that extraction temperature significantly influences the physicochemical and functional properties of CEM, including viscosity, hydration, and polymer organization.[14,15] It has been widely used as a matrix in the development of various drug delivery systems, including tablets,[16,17] transdermal patches,[18] grafted copolymers,[19] and microspheres.[13,20] However, in most reported studies, CEM has been extracted using conventional methods, and limited attention has been given to how extraction conditions influence its physicochemical integrity and subsequent performance in composite drug delivery systems.

Microspheres are versatile, biocompatible, and biodegradable drug carriers designed for controlled, site-specific delivery. Their ability to encapsulate diverse drugs, undergo surface modifications, and overcome physiological barriers makes them ideal for targeted drug delivery.[21] Chemical composition of CEM can vary significantly depending on the extraction method used.[22] Efficient extraction is essential to maximize the potential of CEM. Extraction temperature significantly influences its yield, composition, and quality, with higher temperatures reducing its water-holding capacity.[15] Previous studies by Ghumman *et al.* formulated CEM–alginate microspheres of oxcarbazepine and pregabalin using ionic gelation, where mucilage was extracted through hot-water methods followed by precipitation.[13,20] Nevertheless, the functional performance of such microspheres is highly dependent on polymer extraction and processing conditions, which remain underexplored for CEM–alginate systems.

Tramadol hydrochloride (TrH) is a centrally acting opioid analgesic used to treat moderate to severe pain. Its short biological half-life requires frequent dosing, which can lead to fluctuating plasma levels and dose-related side effects. These limitations make TrH a suitable candidate for sustained-release oral delivery systems. In addition, its pH-dependent and good aqueous solubility make TrH an appropriate model drug for evaluating polymeric microspheres designed for controlled drug release.[23]

In the present study, a distinct formulation strategy was employed using cold-water extraction followed by ethanol precipitation to fabricate TrH-loaded CEM–alginate microspheres. Unlike previously reported CEM–alginate microsphere studies that primarily focus on formulation development using conventionally extracted mucilage, this approach aims to preserve the native physicochemical characteristics of CEM and to examine their influence on microsphere performance. The microspheres were prepared *via* ionic gelation and optimized using a 3^2 central composite design, with calcium chloride as the cross-linking agent. Polymer concentrations of CEM and alginate were selected as independent variables, while encapsulation efficiency and particle size were used as dependent variables.

The optimized formulation was characterized using FTIR, SEM, XRD, and DSC, and evaluated through *in vitro* and *in vivo* drug release studies, along with acute toxicity assessment. The study provides functional insight into how low-temperature-extracted CEM contributes to microsphere formation, encapsulation efficiency, and sustained drug release behavior, thereby addressing a significant gap in the existing literature.

Materials and methods

Materials

Tramadol hydrochloride (The Searle Company Pvt, Ltd Pakistan; ≥99%), *Colocasia esculenta* corms purchased from local market (Voucher No.: UOS-CE-22-15), sodium alginate: M_w 216, CAS-No.: 9005-38-3; ≥99% and ethanol, CAS-No.: 64-17-5; ≥99.5% (Sigma-Aldrich), calcium chloride, CAS No.:10043-52-4; ≥93% (Merck). All other reagents and chemicals were procured from commercial suppliers and were of analytical grade.

Mucilage extraction

A modified version of a previously established method was employed for the extraction and purification of mucilage from *Colocasia esculenta* corms.[14] The major modifications included the use of whole corm slices instead of mechanical blending, lower centrifugation speeds, omission of acetone washing, and cold-water soaking to minimize thermal and mechanical degradation of the mucilage. After washing to remove dust, the

Table 1 Statistical design for CEM–alginate microspheres optimization

Standard		Factors (100 mL)		Responses			
				DEE (%)		Particle size (μm)	
	Run	CEM (g) (X_1)	Alginate (g) (X_2)	Actual	Predicted	Actual	Predicted
12	1	3	3	90.13	90.81	727	728.20
13	2	3	3	90.50	90.81	729	728.20
10	3	3	3	90.80	90.81	726	728.20
7	4	3	1.5	81.07	81.07	676	676.04
6	5	3.7	3	90.30	90.29	719	719.17
4	6	3.5	4	87.60	87.62	724	724.03
8	7	3	4.4	86.00	85.98	712	711.71
1	8	2.5	2	82.10	82.10	672	672.22
5	9	2.2	3	87.40	87.39	682	681.58
2	10	3.5	2	86.80	86.80	697	696.80
3	11	2.5	4	88.20	88.22	695	695.45
11	12	3	3	91.00	90.81	728	728.20
9	13	3	3	91.60	90.81	731	728.20

DDE = drug encapsulation efficiency.

corms were shade-dried. The outer layer was peeled away to yield clear milky-white pieces, which were cut into 1.0 cm slices. Corm slices were soaked in distilled water at 4 °C for 6 hours with occasional stirring and subsequently strained through a muslin cloth. The milky extract was subjected to centrifugation at 3000*g* for 20 minutes to eliminate suspended particulates. Ethanol precipitation was used to isolate the water-soluble fraction of mucilage from the clear solution. Precipitates were washed with ethanol, dried, powdered, screened by 80 mesh sieves, and stored for further investigation in a sealed jar. The extraction yield of mucilage may vary depending on environmental conditions, plant maturity, and batch-to-batch differences; therefore, all extractions were performed under standardized conditions to minimize variability.

Preparation of microspheres by ionotropic gelation

Various blends of CEM–alginate microspheres were developed by the ionotropic gelation method. An aqueous solution of $CaCl_2$ was used as a cross-linking agent. The precisely weighted quantity of CEM was dispersed in distilled water and stirred continuously at 300 rpm on a magnetic stirring machine. Sodium alginate, in a pre-determined amount, was gradually added to the CEM solution with stirring to form a homogeneous mixture. Tramadol hydrochloride (TrH), dissolved in minimal water, was then added to the polymeric suspension. The resulting mixture was extruded dropwise through a 24 G needle into 100 mL of 10% $CaCl_2$ solution. The beads were allowed to gel for 30 minutes, then collected, rinsed with distilled water, and air-dried at room temperature for 24 hours before being transferred to a desiccator until constant weight was achieved.[13]

Experimental design for optimization

A central composite design (CCD) with three levels and two factors was employed using Design-Expert software to statistically optimize the CEM–alginate microspheres. This design, in comparison to other optimization designs, provides a wider and more flexible yet simpler exploration of the design space with fewer runs.[24] By utilizing published literature and preliminary trials, concentrations for CEM (X_1) and alginate (X_2) were selected as independent variables.[25] The factors varied at 3 levels: −1 (low), O (medium) and 1 (high). The dependent variables included encapsulation efficiency (%; Y_1) and mean particle size (Y_2). The experimental design was structured to optimize particle size and drug encapsulation efficiency, utilizing 13 runs to evaluate the influence of independent variables on the measured responses, as shown in Table 1. Each formulation batch was prepared in triplicate and assessed using various statistical models, including linear, 2FI, quadratic, and cubic models. Model fit summaries provided adjusted and predicted R^2 values, *p*-values, and the residual sum of squares.[26,27] The optimal model was selected based on the closest alignment of predicted and adjusted R^2 values and the lowest PRESS and *p*-values. A generalized quadratic equation was employed to describe the relationship between independent variables and response outcomes.

$$Y = b_0 + b_1X_1 + b_2X_2 + b_{11}X_{12} + b_{22}X_{22} + b_{12}X_1X_2 \quad (1)$$

Structural characterization

Fourier transform infrared spectroscopy

The drug–polymer interaction in the TrH-loaded microspheres was examined by FTIR spectroscopy. IR spectral data for CEM, TrH, blank CEM–alginate, and TrH-loaded CEM–alginate microspheres were recorded on an Agilent Cary 630 FTIR.[28]

X-ray diffraction

Powder X-ray diffraction was carried out to analyze the structure of TrH and TrH-loaded microspheres. A scan was run between 5° and 70° at a scan step of 0.02°.[29]

Scanning electron microscopy

SEM was used to evaluate the surface characteristics, shape, porosity, uniformity, and integrity of the microspheres. The particles were fixed on the aluminium stub with two-sided tape. Firstly, the tape was firmly attached to the stub, and then particles were scattered on the other side of the tape. The particles were made conductive by coating with gold by sputtering. Finally, micrographs were captured and saved at different magnifications using the Scanning Electron Microscope JEOL. JSM-5910, Tokyo, Japan.[30]

Thermal analysis (TGA and DSC)

The thermal stability of CEM, TrH, and optimized microsphere formulation was evaluated from 25 °C to 550 °C in a thermal analyzer SDT Q 600. Precisely weighed samples were sealed in aluminium pans, and the temperature was raised at a rate of 10 °C min^{-1} under a nitrogen atmosphere maintained at a flow rate of 10 mL min^{-1} to ensure an inert environment.[31]

Particle size

Fifty dried microspheres were randomly selected, and their diameters were measured using a calibrated optical microscope (Olympus, Tokyo, Japan) to calculate the average particle size.[32]

Drug encapsulation efficiency

Encapsulation efficiency was measured to assess the amount of TrH incorporated into the CEM–alginate microspheres. Precisely weighted 100 mg particles from each formulation were crushed using a pestle and mortar and soaked in 250 mL 7.4 phosphate buffer for about 24 hours at 37 ± 0.5 °C. After 24 hours, the soaked polymeric material was stirred to release drug content, and debris was filtered using Whatman No. 40 paper. Drug encapsulation was measured *via* UV-VIS spectrophotometry at 271 nm (Shimadzu Pharmaspec-1700), and efficiency was calculated accordingly:[33]

$$\text{Encapsulation efficiency}\,(\%) = \frac{\text{encapsulated amount of TrH in a formulation}}{\text{theoretical amount of TrH in a formulation}} \times 100. \quad (2)$$

Swelling studies

Swelling of TrH-loaded CEM–alginate microspheres was evaluated in phosphate buffer (pH 7.4) and 0.1 N HCl (pH 1.2) gravimetrically. Accurately weighted 100 mg of microspheres were placed in 500 mL of each medium at 37 ± 0.5 °C and 50 rpm in a disintegration tester (Pharma Max, Germany). Samples were removed at set intervals, gently dried, and weighed.[26] The swelling index percent was calculated using the following formula:

$$\text{Swelling index}\,(\%) = \frac{W_2 - W_1}{W_1} \times 100 \quad (3)$$

where W_1 is the dry weight of microspheres, while W_2 is the swollen weight.

Degradation studies

The degradation behavior of the optimized formulation was evaluated by placing 100 mg of microspheres in 500 mL of two different media (pH 1.2 and 7.4) in the container of a disintegration tester, maintained at 37 ± 0.5 °C with a stirring speed of 50 rpm. At predetermined time points, the samples were removed, oven-dried, and weighed.[34] The extent of degradation over time was calculated using the following formula:

$$\text{Weight change} = \frac{W_D - W_0}{W_0} \quad (4)$$

W_0 is the initial weight of dry microspheres, and W_D is the final dried weight of microspheres.

In vitro drug release

Drug release from the optimized TrH-loaded CEM–alginate microspheres was studied using a USP-II rotating basket-type dissolution test apparatus (50 rpm, 37 ± 0.5 °C) in 900 mL of buffer (pH 1.2 and 7.4) over 12 hours. Samples (5 mL) were withdrawn at set intervals and replaced with fresh medium. Drug content was measured spectrophotometrically by a UV-VIS spectrophotometer at 271 nm using a standard calibration curve.[31]

The drug release data obtained was used to evaluate the order and release mechanism of TrH from the fabricated microspheres network. Various kinetic models, including zero-order, first-order, Higuchi, Hixson–Crowell, and Korsmeyer–Peppas, were applied to determine the best-fitting model for the obtained release data. The goodness of fit for each model was evaluated using the correlation coefficient (R^2). In the Korsmeyer–Peppas model, the release exponent (n) was used to elucidate the drug release mechanism.[35]

Toxicological analysis

Acute oral toxicity evaluation of CEM–alginate microspheres was carried out on albino rabbits (1.5–2 kg) *via* the oral route. The rabbits were arranged in two groups (n = 3): normal control (Group A) and a group treated with the optimized formulation (Group B). This group size was chosen in line with standard guidelines for preliminary safety assessment. All experimental procedures complied with OECD guidelines and were approved by the Biosafety and Ethical Review Committee, University of Sargodha (Ref: SU/ORIC/394/22/09/2022). Rabbits were housed in well-ventilated, clean cages and given unrestricted access to a standard diet and water for acclimatization. The treatment group received a single oral dose of the formulation at 2000 mg kg^{-1}, while the control group remained untreated. Post-administration, animals from both groups were returned to their cages under standard housing conditions. Daily observations were conducted for signs of morbidity or mortality. Body weight, as well as food and water consumption, were recorded at predefined intervals. After a 14-day observation period, the animals were humanely sacrificed, and major organs were excised, rinsed with saline, weighed, and preserved in 10% formalin for further analysis. Stained organ

sections were microscopically examined and photographed to evaluate histopathological differences between the groups.[36]

In vivo pharmacokinetic study

Albino rabbits (2–2.5 kg) procured from the animal house of the University of Sargodha were used for an *in vivo* pharmacokinetic study. The rabbits were kept in the animal house in hygienic and airy cages. The animals were grouped (n = 10) into control (Group I) and treated (Group II). This group size was selected to ensure sufficient data for assessing drug absorption and plasma concentration profiles.[37] All rabbits underwent overnight fasting with free access to water prior to the start of the experiment. The control group received an aqueous solution of TrH, while the treated group was administered a suspension of the optimized microsphere formulation containing an equivalent dose of the drug (4 mg kg^{-1}) orally. Blood samples (3 mL each) were collected from the jugular vein at predetermined time intervals (1, 2, 3, 4, 6, 8, 10, and 12 hours) and stored in vials for subsequent analysis. Plasma was isolated by centrifuging the collected blood samples at 5000 rpm for 10 minutes. About 1 mL of plasma sample was mixed with 700 μL of acetonitrile to precipitate proteins. The mixture was vortexed for 1 minute, followed by centrifugation at 5000 rpm for 10 minutes. A clear supernatant was obtained by decanting the protein sediment. High-performance liquid chromatography was employed to determine drug concentrations in plasma. The clear plasma containing TrH (100 μL) was injected into the C18 column (4.6 × 250 mm) of the HPLC system (Shimadzu, Japan). The mobile phase used was 0.01 M phosphate buffer and acetonitrile (70 : 30) with a flow rate of 1 mL per minute. A calibration curve with 50, 100, 200, 400, 600, 800, and 1000 ng mL^{-1} dilutions of TrH in methanol was prepared for the quantification of the drug. Pharmacokinetic parameters were determined using a non-compartmental model in PKSolver software.[38]

Results and discussion

Colocasia esculenta mucilage (CEM)

Colocasia esculenta corms are a rich source of mucilage with promising pharmaceutical applications. In this study, cold-water-extracted and ethanol precipitated CEM appeared as a creamy white powder with a yield of 3.78 ± 0.40%, comparable to previous cold extraction reports (3–4.5%), while higher yields are often obtained with hot-water or solvent-assisted methods. However, elevated temperatures can compromise polymer structure, hydration, and functional groups.[39] The cold-extracted CEM exhibited a swelling index of 17.85 ± 1.50, reflecting substantial water uptake and preserved hydrophilic functional groups essential for polymer expansion and gel formation. Cold-water extraction thus preserves the native polysaccharide composition and functional characteristics, including hydroxyl and carboxyl groups, making it particularly suitable for formulation into microspheres and controlled drug delivery systems, where hydration and swelling directly support efficient cross-linking and encapsulation.[14,15]

CEM–alginate microspheres

Physical blending of natural polymers is known to enhance functional properties such as swelling capacity, gel strength, stability, and sustained drug release behavior. Adjusting the polymer ratios can result in unique physicochemical characteristics that influence the encapsulation process and yield diverse drug release profiles.[40] In this work, well-formed and spherical microspheres were obtained by dropping the TrH-loaded CEM and sodium alginate blend into calcium chloride solution, which initiated ionic cross-linking. The mild gelation environment preserved drug stability and facilitated the formation of uniform microspheres with improved morphology compared to previously reported systems.[13,20]

Cold-water extraction better preserves the native functional groups (hydroxyl, uronic acid, and carboxyl moieties) of natural polysaccharides, essential for cross-linking and gel formation.[41,42] These preserved functionalities likely enhanced the cross-linking efficiency with calcium ions, leading to the formation of more uniform and spherical microspheres with improved mechanical integrity. Observations during formulation indicated that optimal CEM concentrations were critical to producing spherical, mechanically stable microspheres with minimal aggregation or deformation. These outcomes demonstrate that cold extraction, combined with controlled polymer ratios, contributes significantly to improved microsphere formation and performance. The physical appearance of optimized microsphere formulation is shown in Fig. 1.

3.1. Optimization

Optimizing experimental design is a fundamental aspect of developing effective drug delivery systems. This study employed a three-level, two-factor central composite design (CCD) to optimize CEM–alginate microspheres. CEM and alginate concentrations were evaluated for their impact on particle size and encapsulation efficiency. Furthermore, ANOVA indicated that CEM–alginate concentrations significantly influenced all responses, with $p < 0.01$. The dependent variables, including particle size and encapsulation efficiency, were analyzed using linear, 2FI, quadratic and cubic models. The quadratic model was selected as the best fit, based on several statistical criteria, including R^2 correlation coefficient, predicted R^2 and PRESS,[43] as shown in Tables 2 and 3. The aliased cubic model was excluded as it provided no meaningful improvement. Statistical validation *via* ANOVA confirmed the adequacy of the regression model, with highly significant p-values (<0.0001) across all responses. Consistency between adjusted and predicted R^2 values, with differences below 0.2, confirms the model's robustness and its predictive accuracy, reflecting a favorable signal-to-noise ratio. Furthermore, this validation affirmed the statistical soundness and suitability of the regression models in describing the relationships between independent and dependent variables. The adequate precision

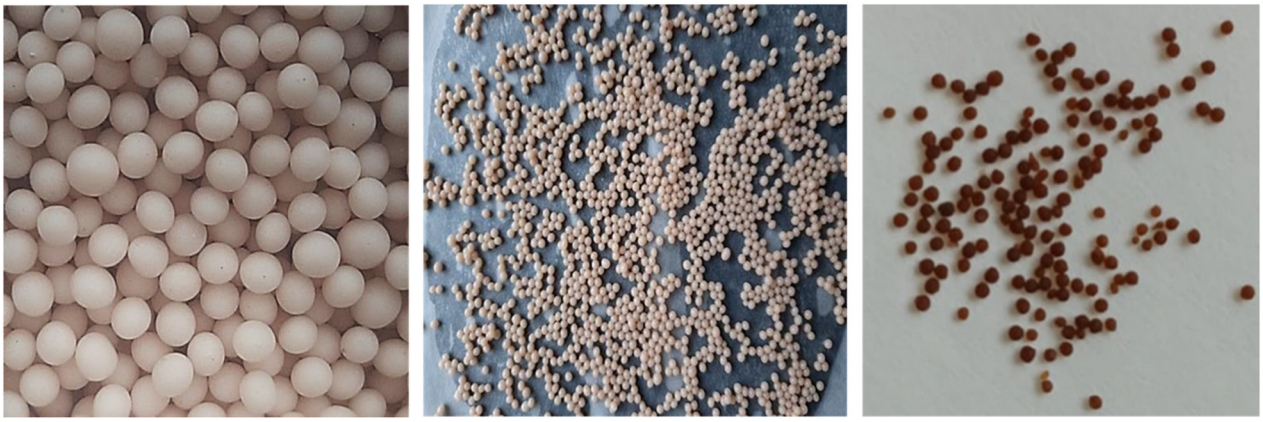

Fig. 1 Physical appearance of optimized TrH-loaded CEM–alginate microspheres prepared by ionic gelation.

Table 2 Fit summary

Source	Sequential p-value	Lack of fit p-value	R^2	Adjusted R^2	Predicted R^2	PRESS	
Response 1: drug encapsulation							
Linear	0.2519	0.0008	0.2410	0.0892	−0.3555	182.58	
2FI	0.4362	0.0007	0.2931	0.0575	−0.5608	210.22	
Quadratic	<0.0001	0.9999	0.9909	0.9845	0.9858	1.91	Suggested
Cubic	0.9987	0.9664	0.9909	0.9783	0.9856	1.94	Aliased
Response 2: particle size							
Linear	0.0419	0.0001	0.4697	0.3636	0.1626	4789.17	
2FI	0.9156	0.0001	0.4704	0.2938	−0.1808	6752.69	
Quadratic	<0.0001	0.9821	0.9973	0.9954	0.9952	27.24	Suggested
Cubic	0.9278	0.8631	0.9974	0.9937	0.9946	31.13	Aliased

Table 3 ANOVA result for quadratic model

Source	Sum of squares	df	Mean square	F-Value	p-Value	
Response 1: drug encapsulation						
Model	133.47	5	26.69	153.17	<0.0001	Significant
A-CEM	8.41	1	8.41	48.24	0.0002	
B-Alginate concentration	24.05	1	24.05	138.02	<0.0001	
AB	7.02	1	7.02	40.29	0.0004	
A^2	6.71	1	6.71	38.52	0.0004	
B^2	92.16	1	92.16	528.82	<0.0001	
Residual	1.22	7	0.1743			
Lack of fit	0.0013	3	0.0004	0.0014	0.9999	Not significant
Pure error	1.22	4	0.3047			
Cor total	134.69	12				
Response 2: particle size						
Model	5703.54	5	1140.71	519.20	<0.0001	Significant
A-CEM	1413.15	1	1413.15	643.21	<0.0001	
B-Alginate concentration	1272.90	1	1272.90	579.37	<0.0001	
AB	4.00	1	4.00	1.82	0.2192	
A^2	1346.49	1	1346.49	612.87	<0.0001	
B^2	2049.05	1	2049.05	932.65	<0.0001	
Residual	15.38	7	2.20			
Lack of fit	0.5792	3	0.1931	0.0522	0.9821	Not significant
Pure error	14.80	4	3.70			
Cor total	5718.92	12				

values for both responses were well above the recommended threshold of >4 *i.e.*, 23.3 for DEE and 37.7 for particle size.[44] The non-significant lack of fit values calculated confirmed the experimental variation captured by replication adequacy. Moreover, the adjusted R^2 values (0.984 and 0.99) were closely aligned with the predicted R^2 values (0.985 and 0.99), indicating minimal error and justifying model validity in explaining the variable relationship. The second-order poly-

nomial equations were utilized to illustrate the mathematical relationship between factors and responses.

$$\text{Drug encapsulation efficiency } (Y_1) = 90.8 + 1.02X_1 + 1.73X_2 - 1.325X_1X_2 - 0.98{X_1}^2 - 3.63{X_2}^2 \quad (5)$$

$$\text{Particle size } (Y_2) = 728.2 + 13.29X_1 + 12.61X_2 + 1.0X_1X_2 - 13.9{X_1}^2 - 17.16{X_2}^2 \quad (6)$$

The magnitude and sign of polynomial terms play a key role in determining how independent factors affect the response. The coefficient indicates how much the response changes when a coded parameter is adjusted, while keeping other variables constant. Positive coefficients represent synergistic effects; negative ones indicate antagonism. In eqn (5) and (6), X_1 and X_2 imply that increasing the concentrations of CEM and alginate increases both the encapsulation efficiency and particle size.[45] Moreover, the negative interaction and quadratic terms indicate the antagonistic effect of X_1 and X_2 at higher concentrations on Y_1 in eqn (5). Similarly, the quadratic terms for X_1 and X_2 indicate a reduction in particle size (Y_2) at higher levels of these factors, as reflected in the eqn (6).

Furthermore, the linear correlation plots of actual *versus* predicted values displayed a strong alignment along a straight line, as shown in Fig. 2, indicating excellent model accuracy and validating its applicability for predicting the behavior of CEM–alginate microspheres. The 3D response surface and 2D contour plots further illustrate the influence of CEM concentration variations on the measured responses. The data indicate that the changes in polymer concentrations significantly influence the response.

Optimization

A desirability-based optimization approach was utilized to develop the optimal CEM–alginate formulation. Initial testing established the target parameters for a microsphere size range of 650–800 μm with maximum drug encapsulation efficiency. The optimized formulation included CEM and alginate in ratios of 3 : 3. The formulation has response values that closely aligned with the desirability score of 0.97. The experimental and software-predicted values of drug encapsulation and particle size were evaluated and compared with software predicted values (Table 4). Moreover, the percentage error was calculated to be 0.77 and 0.33 for drug encapsulation efficiency and particle size, respectively, advocating the validity of the software-generated quadratic model.[26,46]

Structural characterization

Structural characterization of the optimized microspheres by FTIR, XRD, SEM, and thermal analysis was performed to confirm the integrity of cold-extracted CEM, its interaction with alginate, and the effects on morphology, crystallinity, and stability.

Fourier transform infrared spectroscopy

The FTIR spectrum of pure TrH exhibited a broad absorption band at ~3300 cm^{-1}, attributed to O–H stretching, along with characteristic C–H stretching vibrations at 2929 cm^{-1} and 2860 cm^{-1}, confirming the presence of hydroxyl and aliphatic groups. Additional bands in the 1600–650 cm^{-1} region correspond to its fingerprint region, consistent with reported literature.[47]

Pure CEM showed a prominent O–H stretching band at 3263 cm^{-1}, indicative of abundant hydroxyl groups, and a C–H stretching peak at 2926 cm^{-1}. The absorption bands observed between 1700–1600 cm^{-1} were assigned to C=O stretching vibrations, while the peak at 1407 cm^{-1} corresponded to the symmetric stretching of carboxylate (COO^-) groups. The peaks in the 1200–800 cm^{-1} region represent characteristic polysaccharide fingerprint vibrations.[39,48]

In the CEM–alginate blend, the O–H stretching bands shifted to 3330 cm^{-1} and 3318 cm^{-1}, accompanied by slight broadening, indicating the formation of intermolecular hydrogen bonding between hydroxyl groups of CEM and carboxylate groups of alginate. Furthermore, the slight shift of C=O stretching bands from ~1600 cm^{-1} to 1604–1597 cm^{-1} suggests electrostatic interactions and hydrogen bonding between the polymer chains.[49] In the drug-loaded formulation, the absence or reduced intensity of characteristic TrH peaks and their slight shifts toward lower wavenumbers indicate successful incorporation of TrH within the polymeric matrix. These changes suggest that TrH interacts with CEM–alginate primarily through hydrogen bonding, without the formation of new chemical bonds, confirming the compatibility of the drug with the excipients and the physical nature of encapsulation (Fig. 3).[50]

X-ray diffraction

X-ray diffraction analysis of pure TrH (B) displayed several sharp and intense peaks in the 2θ range of 10°–30°, with characteristic reflections observed at approximately 10°, 13°, 16°, 18°, 20°, 25°, and 31°, confirming its crystalline nature. These peaks are consistent with previously reported XRD patterns of crystalline TrH. In contrast, pure CEM (A) exhibited a broad diffraction halo centred on $2\theta \approx 15°–25°$, indicating its predominantly amorphous structure. Notably, no characteristic crystalline peaks of TrH were observed in the optimized CEM–alginate microspheres (C), as shown in Fig. 4. The disappearance of TrH diffraction peaks suggests a loss of crystallinity, indicating that TrH exists in an amorphous or molecularly dispersed state within the polymeric matrix.[51,52] This amorphization may be attributed to polymer–drug interactions and the conditions applied during microsphere fabrication, which are known to suppress drug crystallinity in polymer-based delivery systems.[53]

Scanning electron microscopy

Scanning Electron Microscopy revealed that the TrH-loaded microspheres of CEM–alginate possessed a spherical morphology (Fig. 5). These microspheres displayed rough, irregular surfaces with pores and wrinkles, presumably caused by shrinkage during water loss in the drying process. The uniformly textured irregular surface suggests strong intermolecular interactions between polymer chains and/or with the cross-linking agents used during synthesis.[35,54]

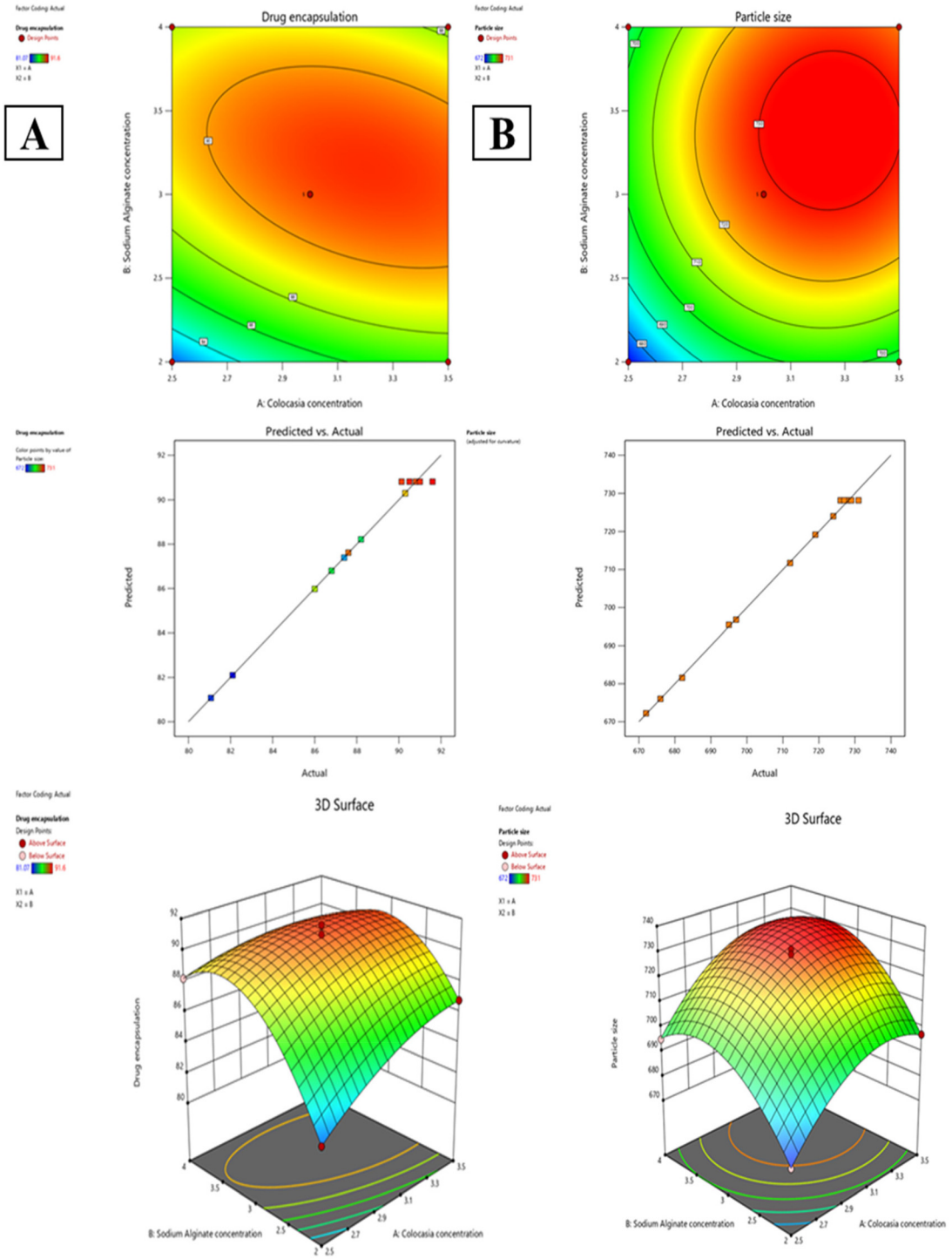

Fig. 2 2-D contour, predicted *vs.* actual and 3-D surface plots; (A) drug encapsulation efficiency; (B) particle size.

Thermal analysis

An overlay of TGA thermograms of TrH, polymers, and optimized formulations of both PAG and CEM is presented in Fig. 6. Thermogravimetric analysis (TGA) of TrH showed that the drug remained stable up to 200 °C, with the greatest weight loss observed between 200 °C and 250 °C.[55] Microspheres of both polymers are more thermally stable than the drug and polymers up to 600 °C.[13]

DSC thermograms (Fig. 7) revealed clear differences in the thermal behavior of the pure polymer and the formulated

Table 4 Formulation optimization

Factor	Goal	Lower limit	Upper limit
Constraints			
X_1: CEM concentration	In range	2.5	3.5
X_2: alginate concentration	In range	2	4
Responses			
Particle size	In range	650	800
Drug encapsulation efficiency	In range	80	95

CEM concentration	Alginate concentration	Drug encapsulation efficiency			Particle size		
		Actual	Predicted	% error	Actual	Predicted	% error
Optimized formulation							
3	3	90.10	90.806	0.77	726	728.2	0.30

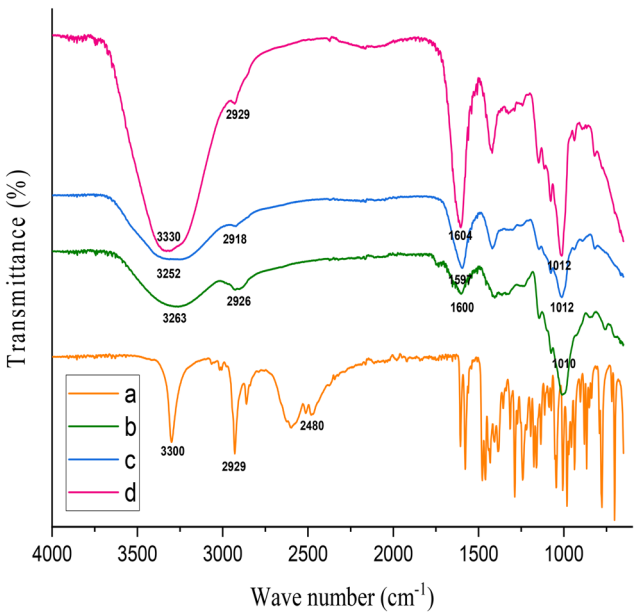

Fig. 3 FTIR results of (a) TrH, (b) pure CEM, (c) blank CEM–alginate microspheres, (d) optimized CEM–alginate microspheres.

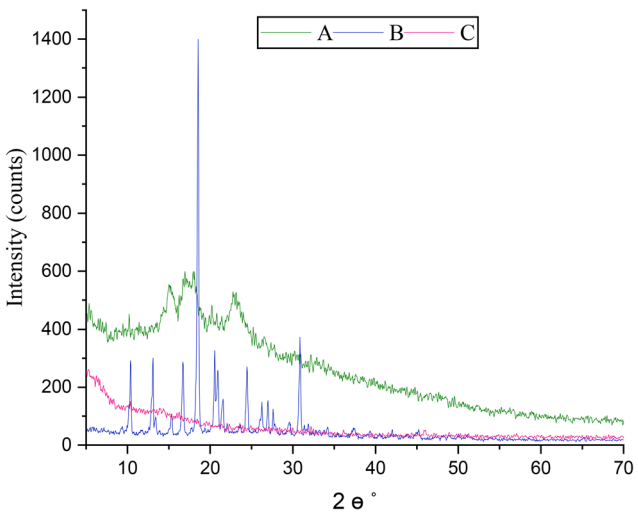

Fig. 4 X-ray diffractogram of A = pure CEM, B = TrH, and C = optimized CEM–alginate microspheres.

microspheres. The DSC profile of pure CEM exhibited broad low-temperature transitions, which are likely due to physical processes such as bound water relaxation and rearrangement of polymer chains typical of hydrophilic polysaccharides rather than chemical degradation. These features reflect the amorphous structure of the mucilage and the presence of hydrogen-bonded moisture within the polymer network.[56] In contrast, the optimized CEM–alginate microspheres showed a smoother thermogram with a more stable baseline, indicating a reduction in enthalpic transitions and restricted molecular mobility. The broadening or absence of sharp transitions suggests the formation of a well-cross-linked polymer matrix, which reinforces structural stability and limits polymer chain flexibility. This thermal stabilization is consistent with previous studies, in which cross-linking with alginate was reported to suppress or shift thermal events, indicating stronger polymer–polymer interactions and enhanced resistance to thermal stress.[57] Overall, these findings suggest that microsphere formation enhances the thermal stability of CEM, supporting its potential application in controlled drug delivery systems.

Particle size

Stable spherical beads are formed by the interaction of carboxylic groups of polymer chains with divalent calcium ions.[58] The mean particle size of prepared CEM–alginate microspheres was observed to range from 672 to 731 μm. The optimized formulation in this study yielded microspheres with an average size of approximately 726 μm using equal concentrations of cold-extracted CEM and alginate (3 g per 100 mL each). The cold-extracted CEM and the balanced polymer blend facilitated the formation of spherical and structurally robust microspheres during ionic gelation. Increasing the CEM concentration increased the particle size due to increased viscosity of the polymeric dispersion, which caused the formation of larger droplets and, consequently, larger microspheres. Larger microspheres generally exhibit slower gastrointestinal transit and prolonged residence time, which can enhance sustained drug release.[59]

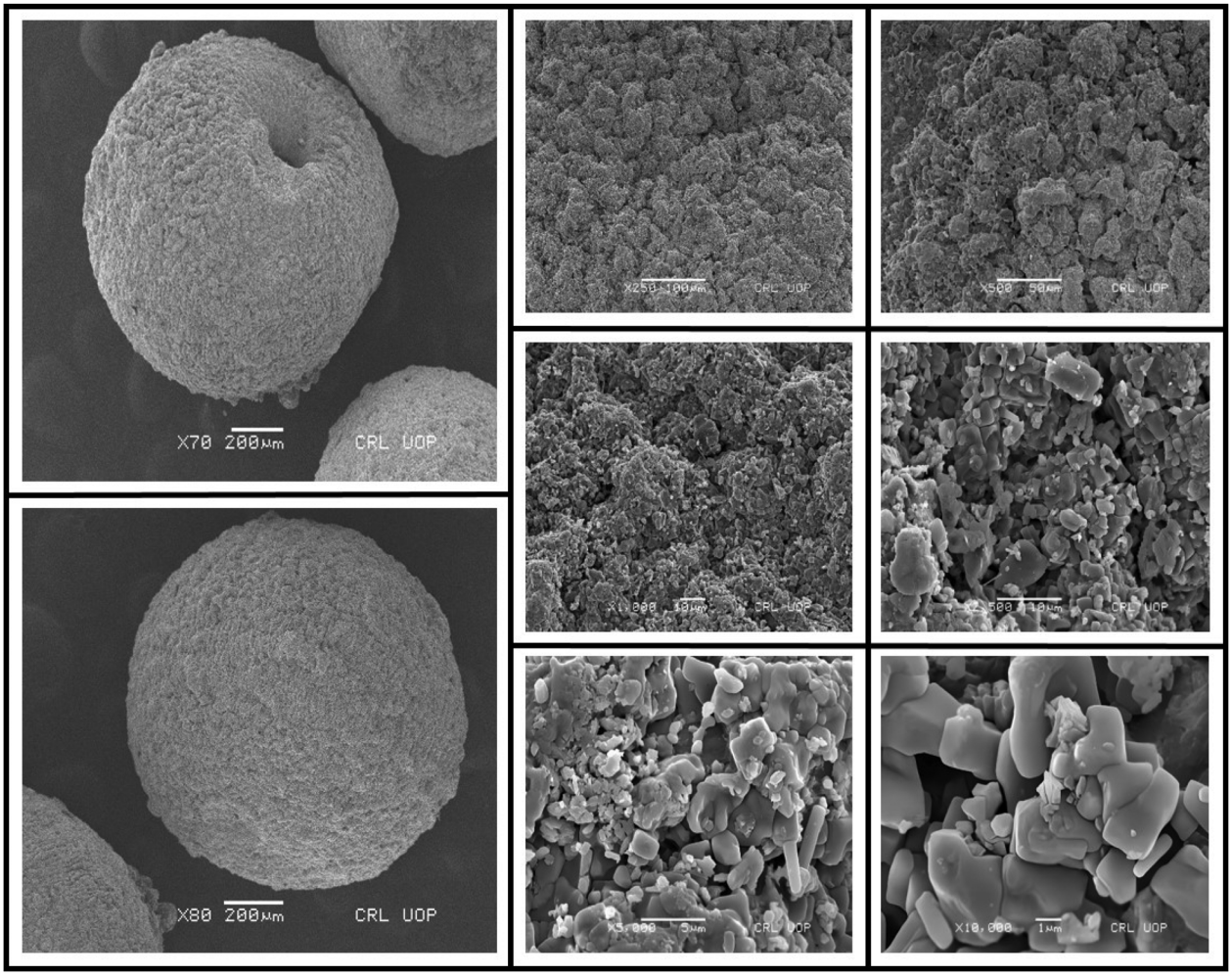

Fig. 5 SEM micrographs of TrH-loaded CEM–alginate blended microspheres. Scale bars: 200, 100, 50, 10, 5, and 1 µm.

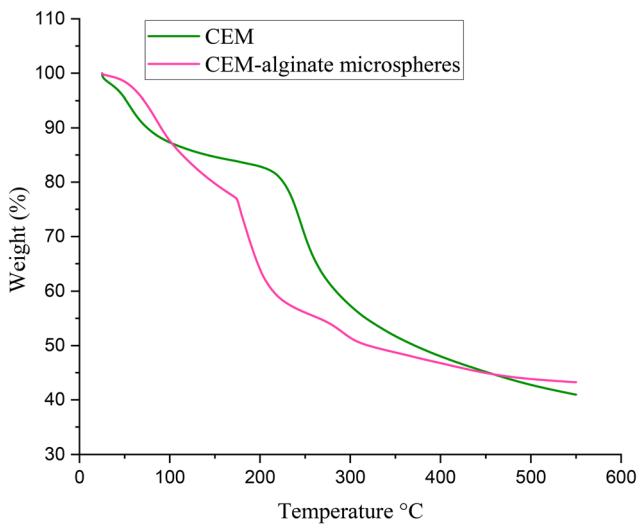

Fig. 6 TGA analysis: CEM and CEM–alginate microspheres.

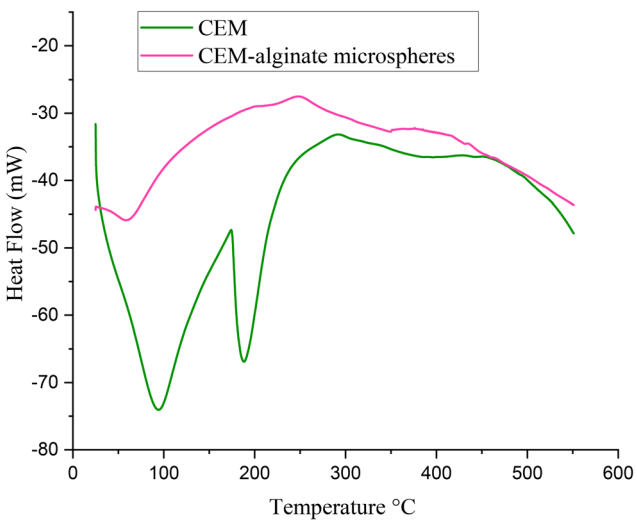

Fig. 7 DSC analysis comparing thermal behavior of CEM and optimized CEM–alginate microspheres.

Drug encapsulation efficiency

The encapsulation efficiency signifies the quantity of drug successfully incorporated into the prepared particles as compared to the quantity initially added. Drug encapsulation capacity is primarily influenced by the physicochemical and morphological features of a polymer-based network. It depends on drug–polymer compatibility and highlights the effectiveness of the fabrication technique in drug loading.[60] The encapsulation efficiency of the CEM–alginate microsphere was 81.07–91.60%, which indicates the good drug entrapment ability of the CEM–alginate polymer system. The encapsulation efficiency of the optimized CEM–alginate microspheres was 90.10%. Data presented in Table 4 demonstrate that variations in CEM and alginate concentrations had a significant influence on encapsulation efficiency. A higher polymer-to-drug ratio enhanced entrapment, likely due to the increased viscosity of the more concentrated blends, which improved the integrity of the cross-linked matrix. Formulations with a greater proportion of CEM exhibited even higher TrH encapsulation, possibly because the enhanced hydration and viscosity of CEM-rich systems minimized drug leaching into the cross-linking medium during curing.[40,61] These findings suggest that the interplay between polymer ratio and compatibility, rather than polymer quantity alone, is critical for maximizing drug entrapment efficiency.

Swelling studies

Water absorption in a polymer-based formulation governs swelling, adhesiveness, drug encapsulation and release, and ultimately polymer degradation.[62] A suitable solvent surrounding the polymeric network penetrates the polymer matrix cause volume changes. Various types of forces, like entropy changes, electrostatic/ionic interactions, hydrophilic/hydrophobic interactions, and osmotic pressure, affect solvent intake by diffusion into the polymer system, causing solvation, polymer chain relaxation, and swelling. This swelling in polymer volume creates gaps between the chains, leading to more mass flow of the surrounding solvent into the system.[63] The swelling behavior of the microspheres is directly correlated with drug release, and both processes are pH-dependent.[64] The alginate-based particles endure chemical and morphological changes at different pHs. At lower pH, the particles shrink to reduce pore size, but above neutral pH, an opposite behavior is observed. The pore sizes increase, and the polymeric particles swell.[65] Optimized CEM–alginate microspheres were assessed for swelling in 0.1 N HCl (pH 1.2) and phosphate buffer (pH 7.4) at 37 °C for 12 hours. It can be inferred from Fig. 8 that the CEM–alginate formulation exhibited pH-responsive swelling behavior, showing a significantly higher swelling index in phosphate buffer (pH 7.4) compared to acidic medium (pH 1.2). This difference in swelling can be attributed to the carboxylic functional groups attached as side chains to the polymers.[66] CEM–alginate microspheres were stable in acidic pH with a noticeably lower swelling ability than phosphate buffer, as reported earlier.[64,67,68] In an acidic medium, maximum swelling was attained in seven hours. The particle shrinkage under acidic pH conditions is the primary factor behind the limited swelling and increased stability of CEM–alginate microspheres.

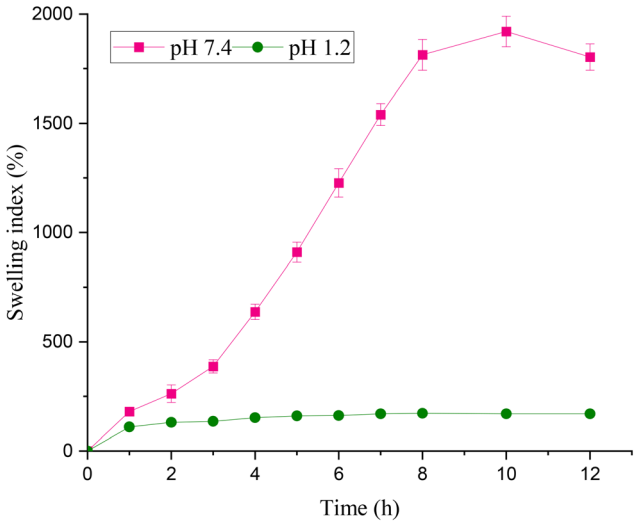

Fig. 8 Swelling index (%) of optimized formulation of CEM–alginate microspheres.

The lower pH suppresses the separation of carboxyl groups in macromolecules. Protonated carboxyl groups create a smaller gel network owing to lesser electrostatic repulsion between alginate chains.[65] At higher pH (7.4) optimized CEM–alginate formulation showed a considerably high swelling index up to ten hours and then started to degrade. At higher pH, ionization of the carboxylic groups present in the polymers (alginate and CEM) occurs, leading to the formation of negatively charged carboxylate ions. This results in electrostatic repulsion between polymer chains. This repulsion pushes the chains apart, facilitating diffusion of medium into the polymer matrix.[67,69] As time passes, calcium ions from cross-linked particles are replaced by sodium ions of the phosphate buffer, which cause disintegration and erosion of the particles. These results suggest that TrH-loaded CEM–alginate particles will show less swelling and stability in the stomach and more swelling in the intestine, making them a potential controlled-release carrier for drug release.[40]

The swelling behavior of the raw CEM was studied in water, while microspheres were evaluated in simulated gastric (pH 1.2) and intestinal (pH 7.4) fluids. Although the testing media differ, a qualitative comparison can still be made: the powder swells rapidly due to direct exposure to water, whereas the microspheres swell more slowly and in a controlled manner because the polymer is incorporated into a cross-linked matrix, which limits water penetration and contributes to sustained release. This highlights the effect of formulation on controlling swelling, even under different pH conditions. Similar observations of slower swelling in cross-linked microspheres compared to raw polymer powder have been reported in previous studies.[70]

Degradation studies

Swelling studies indicated that optimized formulation of CEM–alginate was stable at 1.2, while it degraded gradually at pH 7.4. Microparticle stability and limited erosion arise from protonated carboxylic groups in acidic media, which induce bead shrinkage. In contrast, the phosphate buffer at pH 7.4 induces gradual erosion of the microspheres due to the slow replacement of calcium ions of the cross-linker with sodium ions present in the phosphate buffer.[65] The degradation study was performed in a pH 1.2 and 7.4 buffer. Degradation was very slow at pH 1.2 compared to the phosphate buffer, as shown in Fig. 9. Results of degradation at pH 7.4 proved that CEM incorporation in alginate generated comparatively stable microspheres than sole alginate microspheres, as discussed in our previous reported study.[34]

In vitro drug release

The drug release from polymer-based microspheres is influenced by a complex set of critical factors like properties of polymer (molecular weight, degradation rate) and formulated microspheres (size, morphology and composition), drug–polymer interactions, and selected preparation method.[71,72] The *in vitro* release profile of TrH from the optimized microsphere formulation was systematically investigated and is depicted in Fig. 10 as a cumulative percentage. Within the initial 2 hours in an acidic medium (pH 1.2), the marketed tablet exhibited the maximum release of TrH, whereas the microsphere formulation released only a minimal amount during the same timeframe and conditions. This restrained release is primarily due to the stability of the microspheres in acidic environments, where the unionized state of the carboxyl groups minimizes swelling and thus limits TrH diffusion. Over the subsequent 10 hours, the microspheres showed a progressive increase in drug release, reaching 67.30% by the end of the 12-hour study. This enhanced release is facilitated by greater swelling and diffusion of the drug at elevated pH levels.[35,50] Comparative evaluation of the release profiles clearly demonstrates that the fabricated CEM–alginate microspheres significantly retard the release of TrH.[73] The pH-responsive release behavior of the CEM–alginate system may vary with the physicochemical properties of the incorporated drug and formulation design. Hydrophilic or ionizable drugs may show faster release under intestinal pH, whereas hydrophobic drugs or different matrix architectures may exhibit slower, erosion-controlled release.[74]

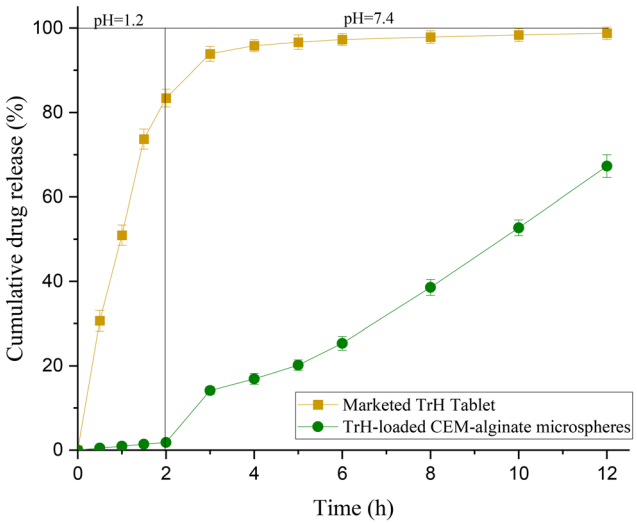

Fig. 10 Cumulative drug release % of Marketed TrH tablet and optimized TrH-loaded CEM–alginate formulations from 1–2 h in pH 1.2 and 3–12 h in pH 7.4.

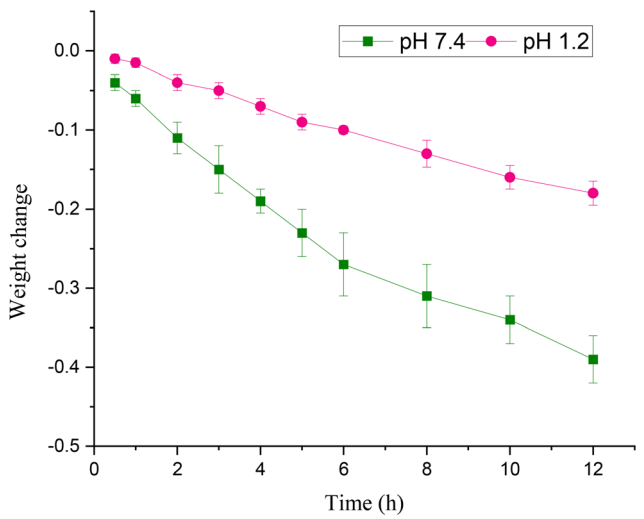

Fig. 9 Degradation of optimized formulation of CEM–alginate microspheres at pH 1.2 and 7.4.

Release kinetics and mechanism of TrH from TrH-loaded CEM–alginate optimized microspheres was examined by fitting the release data of microsphere formulations to several mathematical models to find the most suitable one. Analysis of data modelling results for CEM–alginate beads unveiled that TrH release from these microspheres adopted the Korsmeyer–Peppas model. Results are given in Table 5, which indicates the correlation coefficients, R^2 for the best-fitted model, Korsmeyer–Peppas was found to be 0.9902, and a release exponent value n was 1.369. However, the R^2 value of zero-order (R^2 = 0.9525) was also close to Korsmeyer–Peppas. These results confirm the controlled release of TrH from PAG-alginate microspheres.[34,75] The release exponent (n) obtained from the Korsmeyer–Peppas model indicates a Super Case II transport mechanism rather than simple diffusion-controlled release. This suggests that drug release is predominantly governed by polymer relaxation, swelling, and erosion processes, rather than Fickian diffusion alone. In the optimized microsphere formulation, the interpenetrating three-dimensional network formed by CEM and alginate undergoes significant hydration and chain relaxation upon contact with the dissolution medium. This structural relaxation, coupled with gradual polymer erosion, facilitates sustained drug release. Therefore, the high n value confirms that the release mecha-

Table 5 Results of the best-fitted kinetic model for the *in vitro* release profile of optimized TrH-loaded CEM–alginate microspheres

	Correlation coefficient (R^2)					
Optimized formulation	Zero-order	First-order	Higuchi	Hixson–Crowell	Korsmeyer–Peppas	Release exponent (n)
	0.9525	0.8914	0.6843	0.9128	0.9902	1.369

nism is dominated by polymer matrix relaxation and erosion-driven transport, explaining the prolonged and controlled release behavior of the microspheres.[32]

These findings confirm that polymer ratio, drug solubility, and extraction method collectively influence the release kinetics of CEM–alginate microspheres. Overall, the findings highlight the importance of the extraction technique in determining the functional performance of CEM-based delivery systems. While earlier studies employing hot-extracted CEM have demonstrated its potential in drug encapsulation and sustained release,[13,20] the present work establishes that cold extraction, coupled with ethanol precipitation, preserves the native functional groups of CEM more effectively, leading to well-formed spherical microspheres, higher swelling capacity, and efficient drug entrapment. Although differences in drug type and polymer ratios prevent direct numerical comparisons, the consistent improvements observed in morphology, encapsulation, and release kinetics underline the unique advantages of the cold-extraction strategy for the development of optimized polymeric delivery platforms.

Toxicology study

Given these promising physicochemical and release characteristics, the optimized formulation was further evaluated for its safety through acute toxicity studies. At the end of the two-week trial period, comprehensive examinations were conducted on all rabbits to assess for any signs of illness or toxicity. Food and water consumption, along with body weight, were regularly monitored throughout the duration of the study. All subjects remained active and displayed no signs of morbidity or mortality. No statistically significant variations in body weight were observed between the control and treated groups, as presented in Table 6. Furthermore, food and water consumption patterns remained consistent, and the weights of vital organs showed no notable deviations, suggesting the absence of any treatment-related toxicity over the study period (Table 7).

The hematological, liver, renal, and lipid profile parameters of rabbits treated with CEM–alginate microspheres were comparable to those of the control group (Table 8) and fell within the normal limits reported in previous studies[36] as well as our earlier work with pure mucilage and the same drug in hydrogel formulations[38,76] These findings indicate no treatment-related adverse effects, supporting the safety of the formulation in the acute toxicity study.

Post-dissection organ weights were recorded for all groups. Table 8 indicates similar values across groups, with no histological differences observed (Fig. 11).

Table 6 Summary of acute toxicity indicators in control and treated animals

General observations	Control	CEM–alginate microspheres
Mortality	Nil	Nil
Sign of illness	Nil	Nil
Body weight (g)		
Pretreatment	1217 ± 68	1264 ± 46
Day 1	1222 ± 66	1260 ± 38
Day 7	1233 ± 64	1273 ± 40
Day 14	1249 ± 68	1290 ± 35
water intake (mL)		
Pretreatment	122 ± 3.78	189 ± 11.57
Day 1	125 ± 3.60	192 ± 15.71
Day 7	128 ± 4.16	202 ± 14.42
Day 14	137 ± 9.16	210 ± 12.09
Food intake (g)		
Pretreatment	138 ± 6.24	153 ± 10.96
Day 1	142 ± 7.37	145 ± 11.78
Day 7	147 ± 5.85	159 ± 6.42
Day 14	156 ± 6.65	171 ± 7.76

Table 7 Comparison of hematological and biochemical profiles between control and treated rabbits

Parameters	Control	CEM–alginate microspheres
Hematology		
Hb (g dl^{-1})	13.70 ± 0.62	13.9 ± 0.72
Total WBCs (10^3 μl^{-1})	10.63 ± 0.64	10.43 ± 0.71
RBC (10^6 μl^{-1})	5.83 ± 0.11	5.83 ± 0.23
Platelets (10^3 μl^{-1})	150 ± 7	154 ± 3.60
Liver profile		
AST (U L^{-1})	22.33 ± 4.35	31.67 ± 6.65
ALT (U L^{-1})	81.34 ± 6.02	75 ± 5.50
ALP (U L^{-1})	40.33 ± 4.93	56 ± 7.54
Renal profile		
Urea (mg dl^{-1})	23 ± 3	18.67 ± 2.08
Creatinine (mg dl^{-1})	0.63 ± 0.21	0.93 ± 0.21
Uric acid (mg dl^{-1})	3.73 ± 0.56	3.4 ± 0.30
Lipid profile		
Cholesterol (mg dl^{-1})	104 ± 5.29	93 ± 7.21
Triglyceride (mg dl^{-1})	117 ± 6.08	120 ± 6.81

In vivo drug release

Rabbits were selected as the *in vivo* model due to their suitable body size, ease of repeated blood sampling, and established use in oral pharmacokinetic studies of sustained-release formulations. Their gastrointestinal physiology provides reproducible absorption profiles for tramadol, making them an appropriate preclinical model.[13] Both an aqueous solution of TrH (control) and the optimized drug-loaded CEM–alginate microsphere formulation were administered orally to rabbits at a

Table 8 Vital organ weights: control *vs.* treated groups (g)

Group	Liver	Stomach	Heart	Kidney	Spleen
Control	35.03 ± 0.75	16.93 ± 0.81	3.03 ± 0.40	4.06 ± 0.25	0.43 ± 0.06
CEM–alginate microspheres	35.36 ± 1.05	17.83 ± 1.35	3.86 ± 0.11	4.23 ± 0.56	0.49 ± 0.03

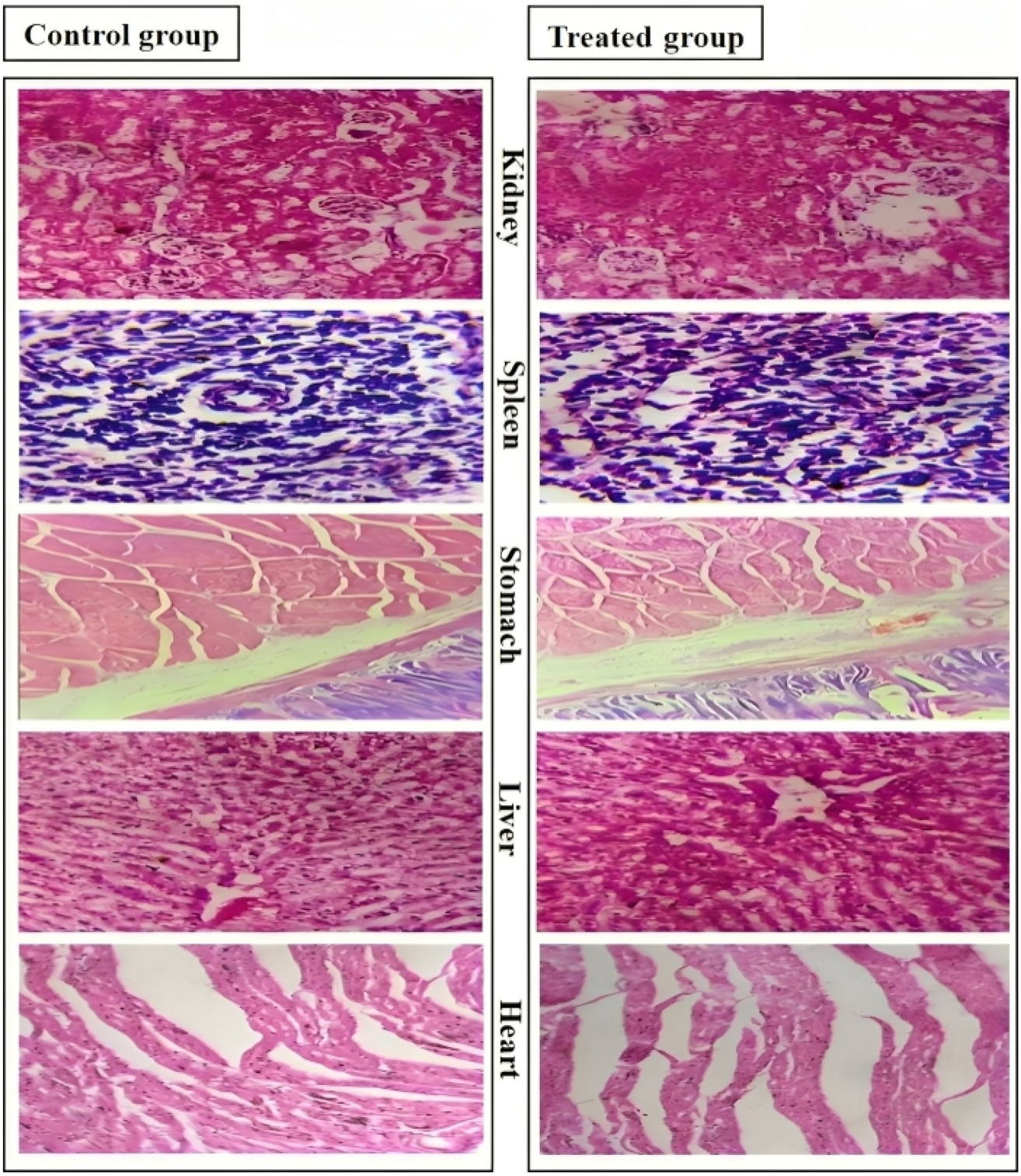

Fig. 11 Histological evaluation of control and optimized TrH-loaded CEM–alginate microspheres treated groups.

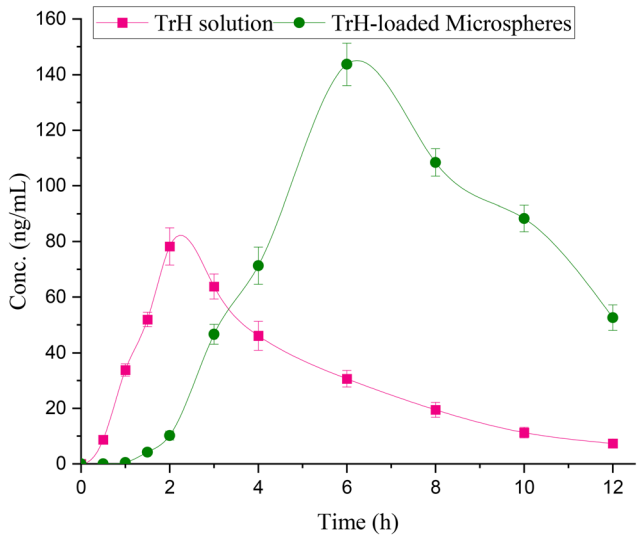

Fig. 12 Overlay of plasma profile of orally administered TrH aqueous solution and optimized CEM–alginate microspheres.

dose of 4 mg per kg body weight. Plasma samples from control and treated groups were analyzed for TrH concentration using a validated HPLC method. The mean plasma concentration-time profiles (Fig. 12) demonstrate that the microsphere formulation significantly delayed the time to reach peak plasma concentration, with T_{max} increasing from 2 h for the aqueous solution to 6 h for the microspheres ($p < 0.05$). This delay confirms the sustained-release behavior of the microsphere system.

Furthermore, the microsphere formulation achieved significantly higher plasma concentrations of TrH compared to the aqueous solution, indicating enhanced systemic exposure. Pharmacokinetic parameters calculated using PKSolver are summarized in Table 9. The optimized microspheres produced a higher C_{max} (143.66 ng mL^{-1}) than the aqueous solution (88.22 ng mL^{-1}, $p < 0.05$). Similarly, the AUC_{0-12} of the microsphere formulation (896.93 ng mL^{-1} h^{-1}) was significantly greater than that of the control (376.39 ng mL^{-1} h^{-1}, $p < 0.05$), confirming improved oral bioavailability.

In addition, the microsphere system significantly prolonged systemic retention of TrH, as reflected by increased half-life (4.30 h *vs.* 2.91 h) and mean residence time (MRT: 10.12 h *vs.* 5.27 h, $p < 0.05$) compared to the aqueous solution. Collectively, these statistically significant differences demonstrate that the CEM–alginate microspheres effectively modulate TrH release, providing sustained plasma levels and prolonged residence time relative to the control formulation.[77,78]

Table 9 Pharmacokinetic evaluation of TrH: aqueous solution *versus* CEM–alginate microsphere formulation

Parameter	Control	CEM–alginate microspheres
C_{max} (ng mL^{-1})	88.22	143.66
T_{max} (h)	2	6
AUC_{0-t} (ng mL^{-1} h^{-1})	376.39	896.93
MRT (h)	5.27	10.12
C_{last} (ng mL^{-1})	7.33	52.58
$T_{1/2}$ (h)	2.91	4.30

Conclusion

The current work signifies the successful formulation and optimization of pH-dependent microspheres employing cold-water extracted and ethanol-precipitated *Colocasia esculenta* mucilage blended with alginate for the sustained delivery of Tramadol hydrochloride. The optimized formulation displayed desirable physicochemical properties, including high encapsulation efficiency, appropriate particle size, and pH-responsive swelling and degradation. Structural investigation confirmed drug–polymer compatibility, and *in vivo* studies proved the formulation's safety, improved bioavailability, and extended drug release. These outcomes highlight the possible implementation of these CEM–alginate microspheres as a productive and biocompatible matrix for extended-release oral drug delivery systems. A limitation of the present study is the lack of a direct experimental comparison between microspheres prepared using hot- and cold-extracted *Colocasia esculenta* mucilage under identical formulation conditions. Future investigations should therefore focus on a systematic, head-to-head comparison using the same drug and polymer ratios to elucidate the influence of extraction temperature on mucilage functionality, microsphere characteristics, and drug release performance. Additionally, future studies could explore the use of this formulation with other active pharmaceutical ingredients (APIs) and assess its commercial scalability, thereby broadening the potential applicability of this delivery system.

Conflicts of interest

There are no conflicts of declare.

Data availability

The data that support the findings of this study are available within the article.

Acknowledgements

Support from the "Centre for Advanced Green Technologies and Innovation (CAGTI)" is greatfully acknowledged.

References

1 H. Park, A. Otte and K. Park, Evolution of drug delivery systems: From 1950 to 2020 and beyond, *J. Controlled Release*, 2022, **342**, 53–65.

2 F. Laffleur and V. Keckeis, Advances in drug delivery systems: Work in progress still needed?, *Int. J. Pharm.*, 2020, **590**, 119912.
3 T. C. Ezike, *et al.*, Advances in drug delivery systems, challenges and future directions, *Heliyon*, 2023, **9**(6), DOI: 10.1016/j.heliyon.2023.e17488.
4 M. Harun-Or-Rashid, *et al.*, Recent advances in micro-and nano-drug delivery systems based on natural and synthetic biomaterials, *Polymers*, 2023, **15**(23), 4563.
5 A. Khan, *et al.*, Nanotechnology Solutions For Advancing Sustainable Development Goals (SDGs): Integrating Nanomaterials For Global Sustainability, *BioNanoScience*, 2025, **15**(4), 1–22.
6 Y. K. Sung and S. W. Kim, Recent advances in polymeric drug delivery systems, *Biomater. Res.*, 2020, **24**(1), 12.
7 M. Anas, *et al.*, Therapeutic potential and agricultural benefits of curcumin: a comprehensive review of health and sustainability applications, *J. Umm Al-Qura Univ. Appl. Sci.*, 2024, 1–16.
8 M. Rishabha, T. Vandana and S. Dharmendra, Techniques of Mucilage and Gum Modification and their Effect on Hydrophilicity and Drug Release, *Recent Pat. Drug Delivery Formulation*, 2020, **14**(3), 214–222.
9 A. Khan, *et al.*, Phytochemical-mediated green synthesis of Silver, Copper, and Ag–Cu bimetallic nanoparticles using peganum harmala demonstrating advanced catalytic, antioxidant, and biomedical applications, *Appl. Biochem. Biotechnol.*, 2025, 1–38.
10 M. S. Amiri, *et al.*, Plant-based gums and mucilages applications in pharmacology and nanomedicine: a review, *Molecules*, 2021, **26**(6), 1770.
11 F. Bibi, *et al.*, Therapeutic applications and mechanism of action of plant-mediated silver nanoparticles, *Pak. J. Bot.*, 2024, **56**(2), 531–540.
12 M. M. Tosif, *et al.*, A comprehensive review on plant-derived mucilage: characterization, functional properties, applications, and its utilization for nanocarrier fabrication, *Polymers*, 2021, **13**(7), 1066.
13 S. A. Ghumman, *et al.*, Taro-corms mucilage-alginate microspheres for the sustained release of pregabalin: In vitro & in vivo evaluation, *Int. J. Biol. Macromol.*, 2019, **139**, 1191–1202.
14 H. Lin and A. S. Huang, Chemical composition and some physical properties of a water-soluble gum in taro (Colocasia esculenta), *Food Chem.*, 1993, **48**(4), 403–409.
15 M. Arici, *et al.*, Effect of extraction temperature of taro mucilage on physicochemical and rheological properties, *J. Food Meas. Charact.*, 2024, **18**(3), 1913–1921.
16 D. Gugulothu, S. K. Choudhary and D. K. Khatri, The extraction and investigation of polysaccharide mucilages for use as excipients in drug delivery systems and their application for developing floating tablets of silymarin, *J. Excipients Food Chem.*, 2021, **12**(4), 70–86.
17 G. Arora, K. Malik and I. Singh, Formulation and evaluation of mucoadhesive matrix tablets of taro gum: Optimization using response surface methodology, *Polim. Med.*, 2011, **41**(2), 23–24.
18 S. Sarkar, *et al.*, Fabrication and optimization of extended-release beads of diclofenac sodium based on Ca++ cross-linked Taro (Colocasia esculenta) stolon polysaccharide and pectin by quality-by-design approach, *Int. J. Biol. Macromol.*, 2024, **271**, 132606.
19 A. H. Mijinyawa, G. Durga and A. Mishra, Isolation, characterization, and microwave assisted surface modification of Colocasia esculenta (L.) Schott mucilage by grafting polylactide, *Int. J. Biol. Macromol.*, 2018, **119**, 1090–1097.
20 S. A. Ghumman, *et al.*, Colocasia esculenta corms mucilage-alginate microspheres of oxcarbazepine: Design, optimization and evaluation, *Acta Pol. Pharm.*, 2017, **74**, 505–517.
21 A. N. Yawalkar, M. A. Pawar and P. R. Vavia, Microspheres for targeted drug delivery-A review on recent applications, *J. Drug Delivery Sci. Technol.*, 2022, **75**, 103659.
22 L. A. Andrade, A. C. da Silva and J. Pereira, Chemical composition of taro mucilage from different extraction techniques found in literature, *Food Chem. Adv.*, 2024, 100648.
23 R. Smyj, X.-P. Wang and F. Han, Tramadol hydrochloride, *Profiles Drug Subst., Excipients, Relat. Methodol.*, 2013, **38**, 463–494.
24 S. Narukulla, *et al.*, Comparative study between the Full Factorial, Box–Behnken, and Central Composite Designs in the optimization of metronidazole immediate release tablet, *Microchem. J.*, 2024, **207**, 111875.
25 S. A. Ghumman, S. Noreen and S. tul Muntaha, Linum usitatissimum seed mucilage-alginate mucoadhesive microspheres of metformin HCl: Fabrication, characterization and evaluation, *Int. J. Biol. Macromol.*, 2020, **155**, 358–368.
26 S. Noreen, *et al.*, Formulation, statistical optimization, and in vivo pharmacodynamics of Cydonia oblonga mucilage/alginate mucoadhesive microspheres for the delivery of metformin HCl, *ACS Omega*, 2023, **8**(6), 5925–5938.
27 V. Pande, *et al.*, Design expert assisted formulation of topical bioadhesive gel of sertaconazole nitrate, *Adv. Pharm. Bull.*, 2013, **4**(2), 121.
28 O. P. Bolade, *et al.*, Dataset on phytochemical screening, FTIR and GC–MS characterisation of Azadirachta indica and Cymbopogon citratus as reducing and stabilising agents for nanoparticles synthesis, *Data Brief*, 2018, **20**, 917–926.
29 A. G. S. Celep, A. Demirkaya and E. K. Solak, Antioxidant and anticancer activities of gallic acid loaded sodium alginate microspheres on colon cancer, *Curr. Appl. Phys.*, 2022, **40**, 30–42.
30 Y. Wu, *et al.*, Mucoadhesive improvement of alginate microspheres as potential gastroretentive delivery carrier by blending with Bletilla striata polysaccharide, *Int. J. Biol. Macromol.*, 2020, **156**, 1191–1201.
31 O. S. Reddy, *et al.*, Curcumin encapsulated dual cross linked sodium alginate/montmorillonite polymeric composite beads for controlled drug delivery, *J. Pharm. Anal.*, 2021, **11**(2), 191–199.
32 P. Kurra, *et al.*, Development and optimization of sustained release mucoadhesive composite beads for colon targeting, *Int. J. Biol. Macromol.*, 2019, **139**, 320–331.

33 A. K. Nayak, D. Pal and K. Santra, Swelling and drug release behavior of metformin HCl-loaded tamarind seed polysaccharide-alginate beads, *Int. J. Biol. Macromol.*, 2016, **82**, 1023–1027.
34 S. Noureen, *et al.*, Prunus armeniaca gum-alginate polymeric microspheres to enhance the bioavailability of tramadol hydrochloride: formulation and evaluation, *Pharmaceutics*, 2022, **14**(5), 916.
35 K. Benfattoum, *et al.*, Formulation characterization and in vitro evaluation of acacia gum–calcium alginate beads for oral drug delivery systems, *Polym. Adv. Technol.*, 2018, **29**(2), 884–895.
36 A. Erum, *et al.*, Acute toxicity studies of a novel excipient arabinoxylan isolated from Ispaghula (Plantago ovata) husk, *Drug Chem. Toxicol.*, 2015, **38**(3), 300–305.
37 S. Noureen, *et al.*, pH-sensitive hydrogel from Colocasia esculenta mucilage for controlled tramadol release, *J. Pharm. Sci.*, 2025, 103973.
38 S. Noureen, *et al.*, A novel pH-responsive hydrogel system based on Prunus armeniaca gum and acrylic acid: Preparation and evaluation as a potential candidate for controlled drug delivery, *Eur. J. Pharm. Sci.*, 2023, **189**, 106555.
39 M. M. Tosif, *et al.*, A concise review on taro mucilage: Extraction techniques, chemical composition, characterization, applications, and health attributes, *Polymers*, 2022, **14**(6), 1163.
40 A. K. Nayak, D. Pal and K. Santra, Tamarind seed polysaccharide–gellan mucoadhesive beads for controlled release of metformin HCl, *Carbohydr. Polym.*, 2014, **103**, 154–163.
41 X. Lu, Changes in the structure of polysaccharides under different extraction methods, *EFood*, 2023, **4**(2), e82.
42 Y. Liu and G. Huang, Extraction and derivatisation of active polysaccharides, *J. Enzyme Inhib. Med. Chem.*, 2019, **34**(1), 1690–1696.
43 G.-y. Li, *et al.*, Formulation optimization of chelerythrine loaded O-carboxymethylchitosan microspheres using response surface methodology, *Int. J. Biol. Macromol.*, 2011, **49**(5), 970–978.
44 M. Kumari and S. K. Gupta, Response surface methodological (RSM) approach for optimizing the removal of trihalomethanes (THMs) and its precursor's by surfactant modified magnetic nanoadsorbents (sMNP)-An endeavor to diminish probable cancer risk, *Sci. Rep.*, 2019, **9**(1), 18339.
45 A. K. Nayak, B. Das and R. Maji, Calcium alginate/gum Arabic beads containing glibenclamide: Development and in vitro characterization, *Int. J. Biol. Macromol.*, 2012, **51**(5), 1070–1078.
46 X.-g. Wu, G. Li and Y.-l. Gao, Optimization of the preparation of nalmefene-loaded sustained-release microspheres using central composite design, *Chem. Pharm. Bull.*, 2006, **54**(7), 977–981.
47 R. Kamel and H. Abbas, Self-assembled carbohydrate hydrogels for prolonged pain management, *Pharm. Dev. Technol.*, 2013, **18**(5), 990–1004.
48 S. M. A. Razavi, *et al.*, Some physicochemical properties of sage (Salvia macrosiphon) seed gum, *Food Hydrocolloids*, 2014, **35**, 453–462.
49 S. Walke, *et al.*, Fabrication of chitosan microspheres using vanillin/TPP dual crosslinkers for protein antigens encapsulation, *Carbohydr. Polym.*, 2015, **128**, 188–198.
50 A. K. Nayak, D. Pal and S. Das, Calcium pectinate-fenugreek seed mucilage mucoadhesive beads for controlled delivery of metformin HCl, *Carbohydr. Polym.*, 2013, **96**(1), 349–357.
51 R. Harris, E. Lecumberri and A. Heras, Chitosan-genipin microspheres for the controlled release of drugs: clarithromycin, tramadol and heparin, *Mar. Drugs*, 2010, **8**(6), 1750–1762.
52 S. Maiti, *et al.*, *Sulfated locust bean gum hydrogel beads for immediate analgesic effect of tramadol hydrochloride*, 2014.
53 S. K. Basu, K. Kavitha and M. Rupeshkumar, Evaluation of ionotropic cross-linked chitosan/gelatin B microspheres of tramadol hydrochloride, *AAPS PharmSciTech*, 2011, **12**, 28–34.
54 R. Kamel, A. Mahmoud and G. El-Feky, Double-phase hydrogel for buccal delivery of tramadol, *Drug Dev. Ind. Pharm.*, 2012, **38**(4), 468–483.
55 P. Kaur, S. Ghildiyal and S. Soni, Development and Evaluation of Hydrodynamically Balanced System of Tramadol Hydrochloride by Using Chitosan and Locust Bean Gum, *J. Intern. Med. Emerg. Res.*, 2020, **1**, 1–20.
56 D. Saha and S. Bhattacharya, Hydrocolloids as thickening and gelling agents in food: a critical review, *J. Food Sci. Technol.*, 2010, **47**(6), 587–597.
57 M. Rinaudo, Main properties and current applications of some polysaccharides as biomaterials, *Polym. Int.*, 2008, **57**(3), 397–430.
58 S. Das, *et al.*, Quality-by-design approach for development of sustained-release multiple-unit beads of lamotrigine based on ion-cross-linked composite of pectin and okra mucilage: An in vitro appraisal, *Int. J. Biol. Macromol.*, 2020, **163**, 842–853.
59 M. S. Hasnain, *et al.*, Isolation and characterization of Linum usitatisimum polysaccharide to prepare mucoadhesive beads of diclofenac sodium, *Int. J. Biol. Macromol.*, 2018, **116**, 162–172.
60 E. Freitas, *et al.*, Application of experimental design to evaluate the incorporation of naproxen into sericin/alginate particles prepared by ionic gelation technique, *Chem. Eng. Sci.*, 2021, **229**, 116101.
61 S. Pardeshi, *et al.*, Preparation and characterization of sustained release pirfenidone loaded microparticles for pulmonary drug delivery: Spray drying approach, *Drying Technol.*, 2020, **39**(3), 337–347.
62 F. I. Boni, F. G. Prezotti and B. S. F. Cury, Gellan gum microspheres crosslinked with trivalent ion: Effect of polymer and crosslinker concentrations on drug release and mucoadhesive properties, *Drug Dev. Ind. Pharm.*, 2016, **42**(8), 1283–1290.
63 S. Borandeh, *et al.*, Polymeric drug delivery systems by additive manufacturing, *Adv. Drug Delivery Rev.*, 2021, **173**, 349–373.

64 K. Yari, I. Akbari and S. A. V. Yazdi, Development and evaluation of sodium alginate-basil seeds mucilage beads as a suitable carrier for controlled release of metformin, *Int. J. Biol. Macromol.*, 2020, **159**, 1–10.
65 R. Abka-Khajouei, *et al.*, Structures, properties and applications of alginates, *Mar. Drugs*, 2022, **20**(6), 364.
66 J. Singh and P. Nayak, pH–responsive polymers for drug delivery: trends and opportunities, *J. Polym. Sci.*, 2023, **61**(22), 2828–2850.
67 H. H. Gadalla, *et al.*, Colon-targeting of progesterone using hybrid polymeric microspheres improves its bioavailability and in vivo biological efficacy, *Int. J. Pharm.*, 2020, **577**, 119070.
68 S. A. Ghumman, *et al.*, Formulation and evaluation of quince seeds mucilage–sodium alginate microspheres for sustained delivery of cefixime and its toxicological studies, *Arabian J. Chem.*, 2022, **15**(6), 103811.
69 H. Andishmand, *et al.*, Pectin-zinc-chitosan-polyethylene glycol colloidal nano-suspension as a food grade carrier for colon targeted delivery of resveratrol, *Int. J. Biol. Macromol.*, 2017, **97**, 16–22.
70 A. Raizaday, *et al.*, Formulation and evaluation of pH sensitive microspheres of N-succinyl chitosan for the treatment of diverticulitis, *Cellul. Chem. Technol.*, 2015, **49**(1), 41–50.
71 R. Bhujel, *et al.*, Practical quality attributes of polymeric microparticles with current understanding and future perspectives, *J. Drug Delivery Sci. Technol.*, 2021, **64**, 102608.
72 A. Khan, *et al.*, Eco-friendly synthesis of copper oxide-silver bimetallic nanoparticles using Withania coagulans: Characterization and biomedical potential through antioxidant, antibacterial, and catalytic activities, *Inorg. Chem. Commun.*, 2025, 115131.
73 O. J. Olayemi, Y. E. Apeji and C. Y. Isimi, Formulation and evaluation of Cyperus esculentus (Tiger Nut) starch-alginate microbeads in the oral delivery of ibuprofen, *J. Pharm. Innovation*, 2020, 1–10.
74 G. Kocak, C. Tuncer and V. Bütün, pH-Responsive polymers, *Polym. Chem.*, 2017, **8**(1), 144–176.
75 S. Jusu, *et al.*, Drug-encapsulated blend of PLGA-PEG microspheres: in vitro and in vivo study of the effects of localized/targeted drug delivery on the treatment of triple-negative breast cancer, *Sci. Rep.*, 2020, **10**(1), 14188.
76 S. Noureen, *et al.*, Maximizing the extraction yield of plant gum exudate using response surface methodology and artificial neural networking and pharmacological characterization, *Sci. Rep.*, 2023, **13**(1), 10954.
77 M. N. Aamir, *et al.*, Development and in vitro–in vivo relationship of controlled-release microparticles loaded with tramadol hydrochloride, *Int. J. Pharm.*, 2011, **407**(1–2), 38–43.
78 B. D. Kevadiya, *et al.*, pH responsive MMT/acrylamide super composite hydrogel: characterization, anticancer drug reservoir and controlled release property, *Biochem. Biophys.*, 2013, **1**(3), 43–60.